Available online at www.sciencedirect.com
ScienceDirect
Polymer 48 (2007) 3893–3901
polymer
www.elsevier.com/locate/polymer

Computational modeling of biodegradable blends of starch amylose and poly-propylene carbonate

S.S. Joshi, A.M. Mebel*

Department of Chemistry and Biochemistry, Florida International University, University Park, 11200 SW 8th Street, Miami, FL 33199, USA

Received 13 February 2007; received in revised form 19 April 2007; accepted 20 April 2007
Available online 29 April 2007

Abstract

The current study investigates the nature of interactions between starch (amylose portion) and poly-propylene carbonate by employing DFT based B3LYP and semi-empirical AM1 and PM3 methods on five complexes. The computed negative binding energies confirm the stability of the complexes. Favorable interactions between amylose and poly-propylene carbonate were indicated by the formation of hydrogen bonds. The number of hydrogen bonds identified per poly-propylene carbonate monomer attains a saturation value of 0.57 for AM1 and 0.51 for PM3 for larger complexes. The average binding energy per hydrogen bond was computed to be −12.76 kJ/mol for AM1 and −9.79 kJ/mol for PM3 method. The decrease in the computed vibrational frequencies of the hydroxyl OH and carbonyl C═O frequencies of the complexes agrees qualitatively with experimental results, further confirming the presence of favorable interactions. Molecular modeling was thus successful in providing useful insight into the nature of interactions between starch and PPC.

Keywords: Starch; Composites; Quantum chemical modeling

1. Introduction

A substantial portion of plastic products is manufactured primarily from petroleum-based synthetic polymers. The disposal of these plastic wastes poses serious environmental problems due to their persistent nature, as they are not easily degraded in a landfill. In addition, availability of landfill sites is diminishing and landfills are also prone to leakage of toxic chemicals, which may contaminate groundwater. Another widely practiced disposal technique is incineration (burning of wastes), which is known to generate toxic air pollution. Also, as the petroleum resources are rapidly becoming scarce, there is an urgent need to design and synthesize plastic substitutes, which are easily degraded without posing any serious environmental problems. Biodegradable polymers offer a promising alternative to petroleum-based polymers that are renewable, environmental friendly and can be readily degraded in a natural environment.

Recent research efforts to improve the performance and properties of the plastic polymeric materials focus on blending of polymers with starch [1–5]. Starch is synthesized in granules as a food source in most plant cells; it is a mixture of amylose and amylopectin, both of which are polymers of α-D-glucose units. Starch is inexpensive and is found abundantly in nature, and together with its well known biodegradable properties may offer a potential substitute for petroleum-based synthetic plastics. Starch, by itself, has severe limitations due to its water solubility, poor mechanical properties and brittleness as compared to those of synthetic plastics [6–8]. To overcome these impediments while retaining the biodegradability, blending of starch with other polymers has been widely practiced [9–22].

This research study focuses on the blend of starch and poly-propylene carbonate (PPC). Poly-propylene carbonate, a polymer made from carbon dioxide and propylene oxide, has high tensile strength and Young's modulus. The molecular structure

* Corresponding author. Tel.: +1 305 348 1945; fax: +1 305 348 3772.
E-mail address: mebela@fiu.edu (A.M. Mebel).

0032-3861/$ - see front matter © 2007 Elsevier Ltd. All rights reserved.
doi:10.1016/j.polymer.2007.04.059

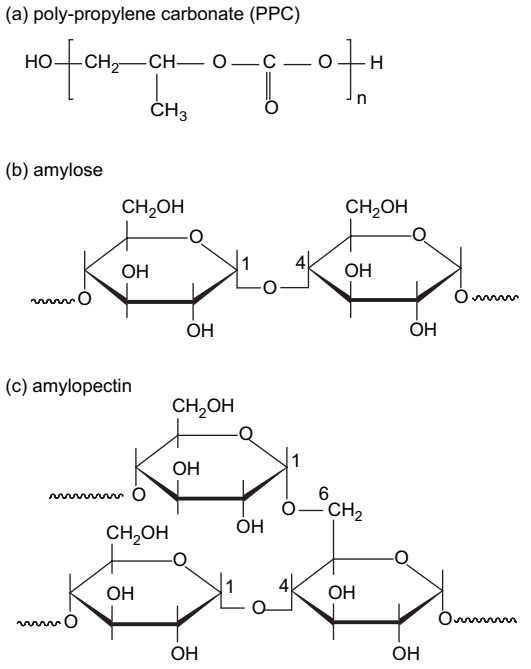

Fig. 1. Structure of (a) poly-propylene carbonate (PPC), (b) amylose, and (c) amylopectin.

of PPC is illustrated in Fig. 1(a). Previous studies have confirmed that incorporation of PPC in starch has significantly improved the mechanical properties of starch such as tensile strength and stiffness [23].

Improved mechanical properties can be realized only if efficient load transfer exists between the constituent polymers. Favorable molecular interactions can improve the load transfer via bonded or non-bonded means. Thus, interfacial interactions between the constituent polymers strongly influence the mechanical properties of the blend. Even with extensive experimental data available [24–26] on interactions of polymer blends, the exact nature of the molecular interactions involved are difficult to construe. A number of theoretical methods such as an integral equation theory [27,28], lattice theory [29] and lattice cluster theory [30,31] have been developed to model polymer blends. Although these methods make the study of larger systems feasible, or the study of smaller systems fast, the underlying assumptions render a trade-off in accuracy by disregarding the presence of discrete molecular structure of matter. Quantum mechanical calculations, on the other hand, involve the solution of Schrödinger's equation for the molecular system and are suitable to investigate the molecular interactions between the polymer blends. Molecular modeling employing semi-empirical methods was found to be successful in studying hydrogen bonding interactions between polyamide-6 and polyurethane polymers [32]. To date, little reported work has been performed on the theoretical molecular modeling of the interactions between starch and PPC. The aim of this study is to determine the compatibility of starch (specifically the amylose portion) and PPC by means of molecular modeling and hence to better understand the molecular nature of interactions between the two constituent polymers at the molecular level. To this purpose, five pairs of complexes consisting of increasing numbers of amylose and PPC monomers have been studied.

The theoretical calculations presented here involve the determination of optimal geometries and relative energetics (binding energy per unit structure) of the blended polymers. Calculations of vibrational frequencies have also been performed and some qualitative comparison with experimental results is also made. These calculations provide considerable insight into the nature of bonding between the polymers as well as ascertain the capability of quantum mechanical methods to model similar interactions.

2. Computational methodology

2.1. Molecular system under consideration

As mentioned earlier, starch is a mixture of amylose and amylopectin, both of which are polymers of α-D-glucose units. Amylose is a linear polymer with glucose monomer units connected with α-1 → 4 linkages (Fig. 1(b)). Amylopectin, on the other hand, has branch points approximately every 20 glucose units along the main chain where short side chains of glucose units are connected by α-1 → 6 linkages (Fig. 1(c)). Thus, amylopectin differs from amylose in being highly branched. For the present study, we consider only the amylose portion of starch for modeling purposes to keep the model computationally manageable, assuming that the nature of the molecular interactions between PPC and amylose would remain qualitatively similar to those between amylopectin and PPC. Keeping this in mind, the following five pairs of complexes of amylose with PPC of increasing number of monomers were analyzed for modeling purposes:

1. 1 amylose–1 PPC (1A:1P),
2. 5 amylose–5 PPC (5A:5P),
3. 10 amylose–10 PPC (10A:10P),
4. 15 amylose–13 PPC (15A:13P),
5. 20 amylose–17 PPC (20A:17P).

To be specific, the first system (1 amylose–1 PPC) consists of one monomer of amylose and PPC each, represented as 1A:1P in shorthand notation. The remaining systems follow the same notation.

2.2. Computational methods

Quantum mechanical modeling methods are the most fundamental and accurate theoretical tools available to predict molecular properties as they treat molecules as collections of nuclei and electrons. Quantum mechanical models are based on the Schrödinger equation, solution to which gives molecular structure and energy. Quantum mechanical (QM) calculations based on density functional theory (DFT) contain no adjustable parameters and solve the Schrödinger equation

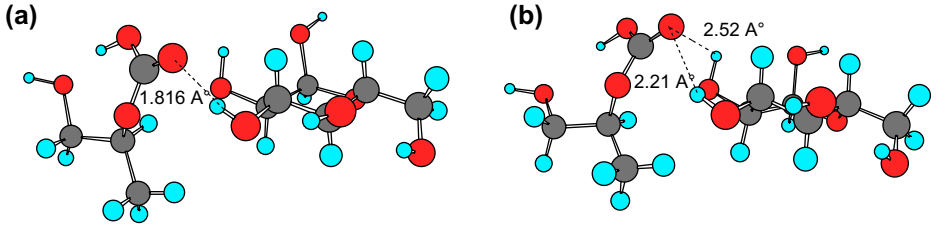

Fig. 2. Geometrically optimized structures of 1A:1P complexes at (a) B3LYP and (b) AM1 levels.

making some reasonable approximations. As QM based DFT calculations are exceedingly computationally expensive, the present study considers only one (1 Amylose−1 PPC) of the five complexes with the smallest number of atoms amenable for the DFT calculation. Semi-empirical methods (AM1 and PM3) [33,34] are employed for the calculations of the remaining four complexes of relatively larger sizes. Semi-empirical methods make use of several experimental data based parameters for the elements to render the solution of Schrödinger equation computationally fast.

2.3. Computational strategy

The following procedure was followed for the geometry optimization of the first complex (1A:1P).

In order to obtain reliable initial geometries, geometry optimization of one amylose monomer, one PPC monomer and different conformations of the corresponding complex (1A:1P) was first performed with molecular mechanics (MM+) force field using Hyperchem version 7.51 [35]. The lowest energy conformation structure was then used as the initial geometry for the more accurate DFT (B3LYP) [36–38] and semi-empirical methods (AM1 and PM3) to yield the binding energies of the corresponding complexes using the Gaussian 98 program package [39]. The magnitude of the energy change is a measure of the driving force towards complexation, a higher negative value denoting a thermodynamically favorable complex.

The optimized structured for this 1A:1P system was repeated five times and was used as an initial structure for the geometry optimization of the 5A:5P system at the AM1 and PM3 levels of theory. The rest of the three systems were optimized in a similar fashion. The geometrically optimized structures for all the five complexes at different levels of theory are depicted in Figs. 2–6.

Vibrational frequencies were computed for the individual amylose and PPC molecules along with their corresponding complexes for 1A:1P and 5A:5P systems at the same respective levels of theory to enable qualitative comparison with experimental IR spectra. The frequency analysis also helps to confirm the located stationary points as true minima (all eigenvalues of the Hessian matrix are positive).

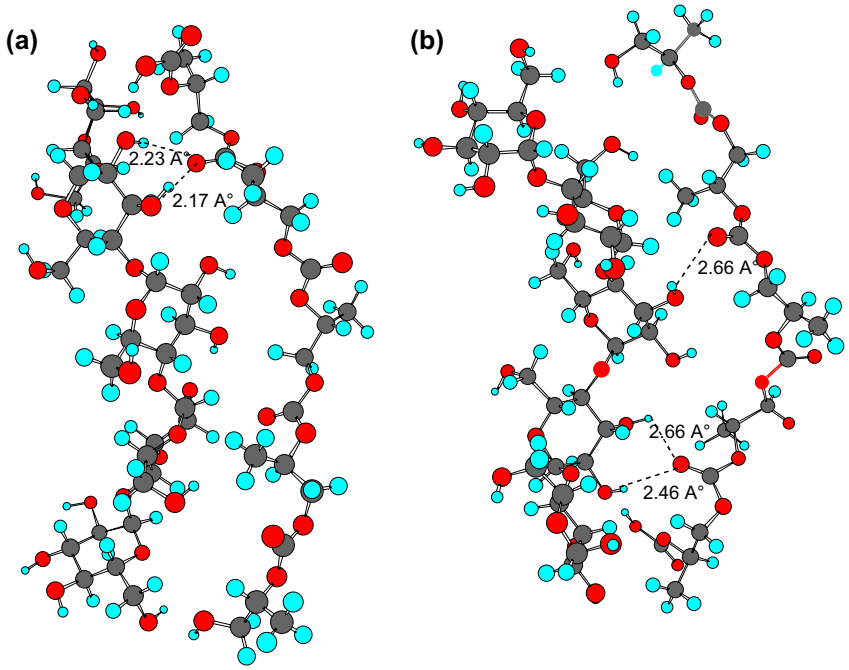

Fig. 3. Geometrically optimized structures of 5A:5P complexes at (a) AM1 and (b) PM3 levels.

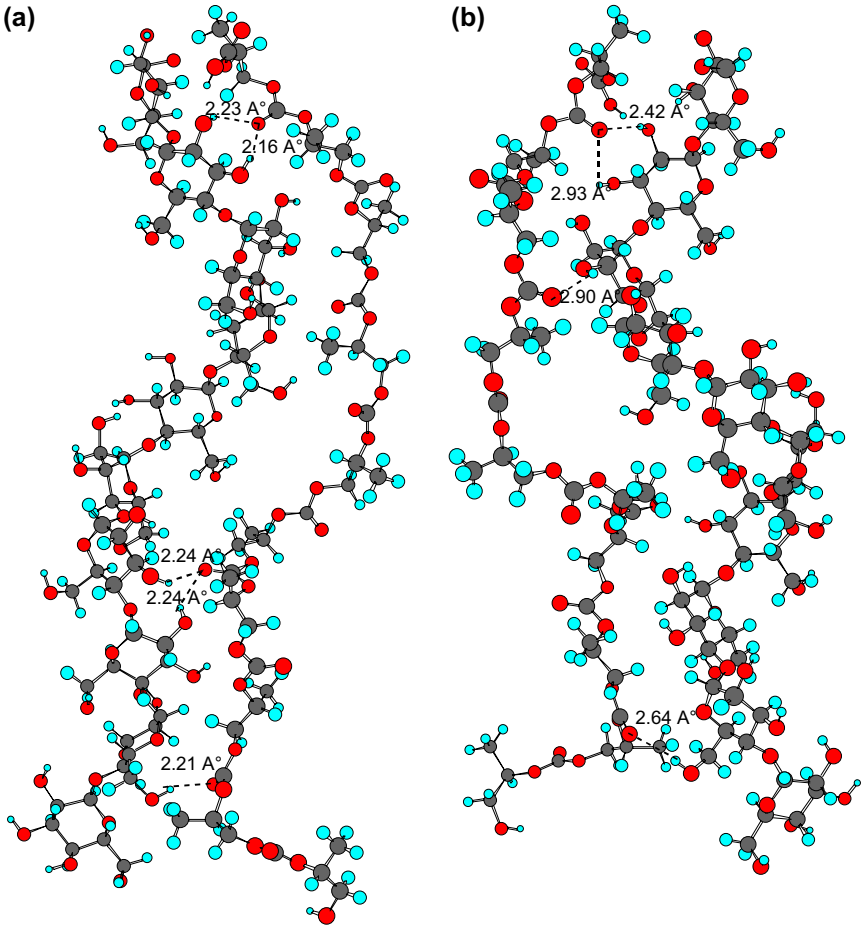

Fig. 4. Geometrically optimized structures of 10A:10P complexes at (a) AM1 and (b) PM3 levels.

3. Results and discussion

3.1. Binding energy

The binding energy of each complex was calculated using the following formula:

$$\Delta E = E_{\text{complex}} - \left(E_{\text{amylose}} + E_{\text{PPC}}\right)$$

Here, E_{complex}, E_{amylose} and E_{PPC} represent total energies of the amylose–PPC complex, the individual amylose and PPC molecules, respectively. The computed AM1, PM3 and B3LYP binding energies are presented in Table 1.

B3LYP with 6-31G basis set was applied to perform only the geometry optimization of the 1A:1P system and single point energy calculation of the 5A:5P systems as the remaining three larger systems are too large in terms of computational demands. The negative energies imply a favorable interaction between the two polymers. The AM1 energies show an increasing trend with increasing polymer length, although the last two systems depict a reverse behavior. A similar distinct trend is absent with the PM3 energies. Overall, we can conclude that the interactions between the two polymers are energetically favorable. Also, as the binding energies increase with the polymer length (at least at the AM1 level), the interaction between the polymers increases with increasing polymer lengths.

3.2. Hydrogen bonding

Amylose has a vast number of hydroxyl OH groups which could favorably interact with the carbonyl C=O group of PPC in a non-bonded fashion. Careful inspection of the optimized geometric structures of all the five complexes shows ample evidence of the interactions between the carbonyl oxygen of PPC and hydroxyl hydrogen of the amylose monomer via hydrogen bonds (hydrogen bonds are shown schematically by dashed lines for some complexes in Figs. 2–4). These intermolecular hydrogen bonds explain the driving forces responsible for the formation of stable complexes.

The hydrogen bond here is defined as an O–H/O interaction in which the O–H distance is less than or equal to 3.0 Å and the angle at H is greater than 90°. Total number of hydrogen bonds identified, average hydrogen bond distance, number of hydrogen bonds per PPC monomer and average binding energy per hydrogen bond obtained from the AM1 and PM3 computations of geometrically optimized structures of all the five complexes are presented in Table 2.

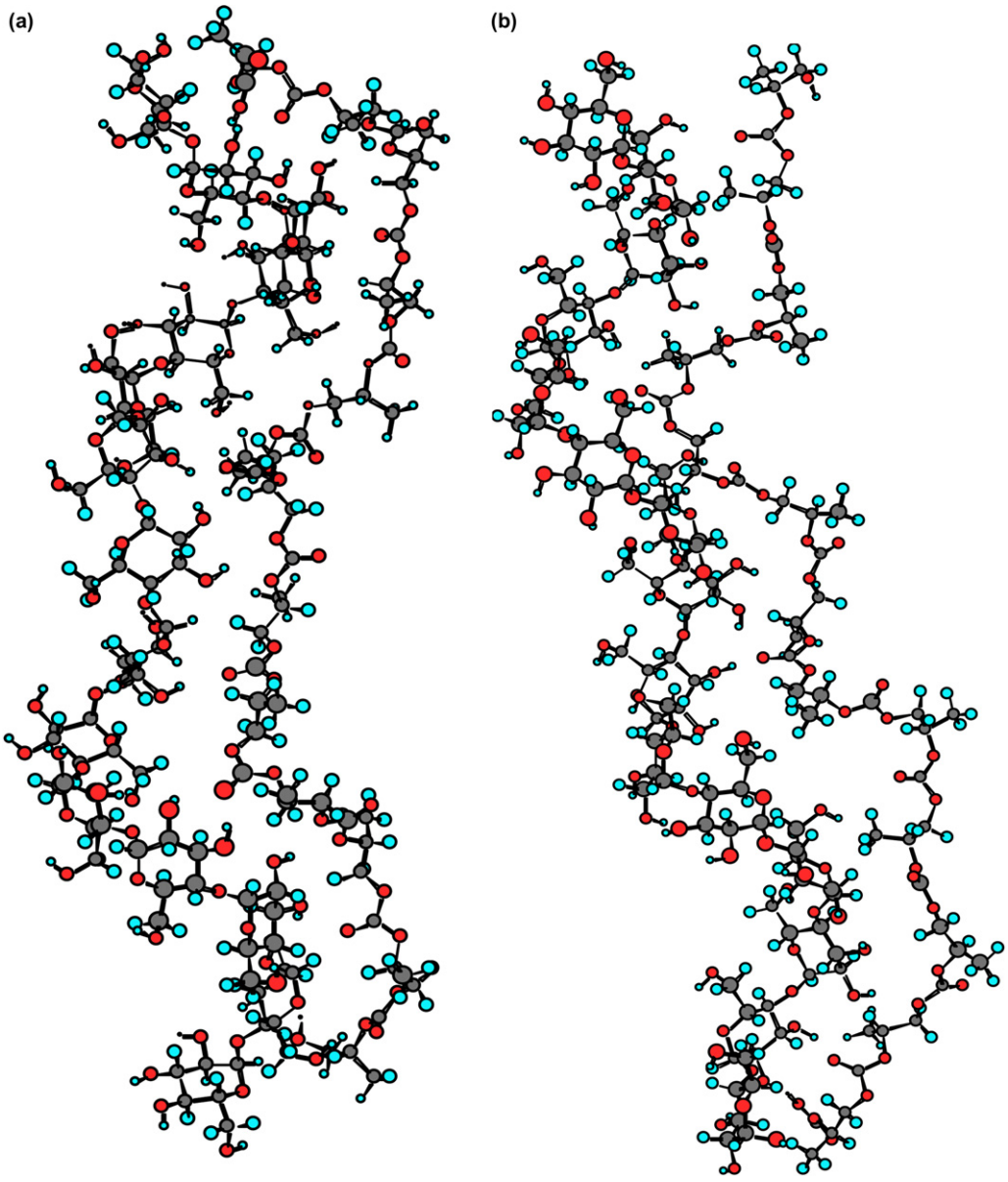

Fig. 5. Geometrically optimized structures of 15A:13P complexes at (a) AM1 and (b) PM3 levels.

Average hydrogen bond distance for each complex is computed by using the following formula:

Average hydrogen bond distance

$$= (\text{Sum of all individual hydrogen bond distances})/N.$$

Here, N is the total number of hydrogen bonds identified in a system.

The number of hydrogen bonds per PPC monomer for each complex is computed using the following formula:

Number of hydrogen bonds per PPC monomer

$$= N/\text{Number of PPC monomers}.$$

PM3 results show that the number of hydrogen bonds identified per PPC monomer decreases as the length of the complex increases and eventually reaches an average saturation value of 0.51 for larger systems (10A:10P, 15A:13P, and 20A:17P). While a distinct decreasing trend may not be present among the AM1 results, nevertheless it is evident that for the larger systems (10A:10P, 15A:13P and 20A:17P) the number of hydrogen bonds per PPC monomer reaches an average saturation value of 0.57, which is relatively less compared to the smaller systems. A close inspection of the optimized geometric structures of the complexes reveals that for some portions of the larger systems (10A:10P, 15A:13P and 20A:17P) steric hindrance and unfavorable geometry render the hydroxyl OH and the carbonyl C═O groups far from each other, which may be responsible for the above behavior.

Finally, the average binding energy per hydrogen bond for each complex is computed by using the following formula:

$$\text{Average binding energy per hydrogen bond} = \Delta E/N.$$

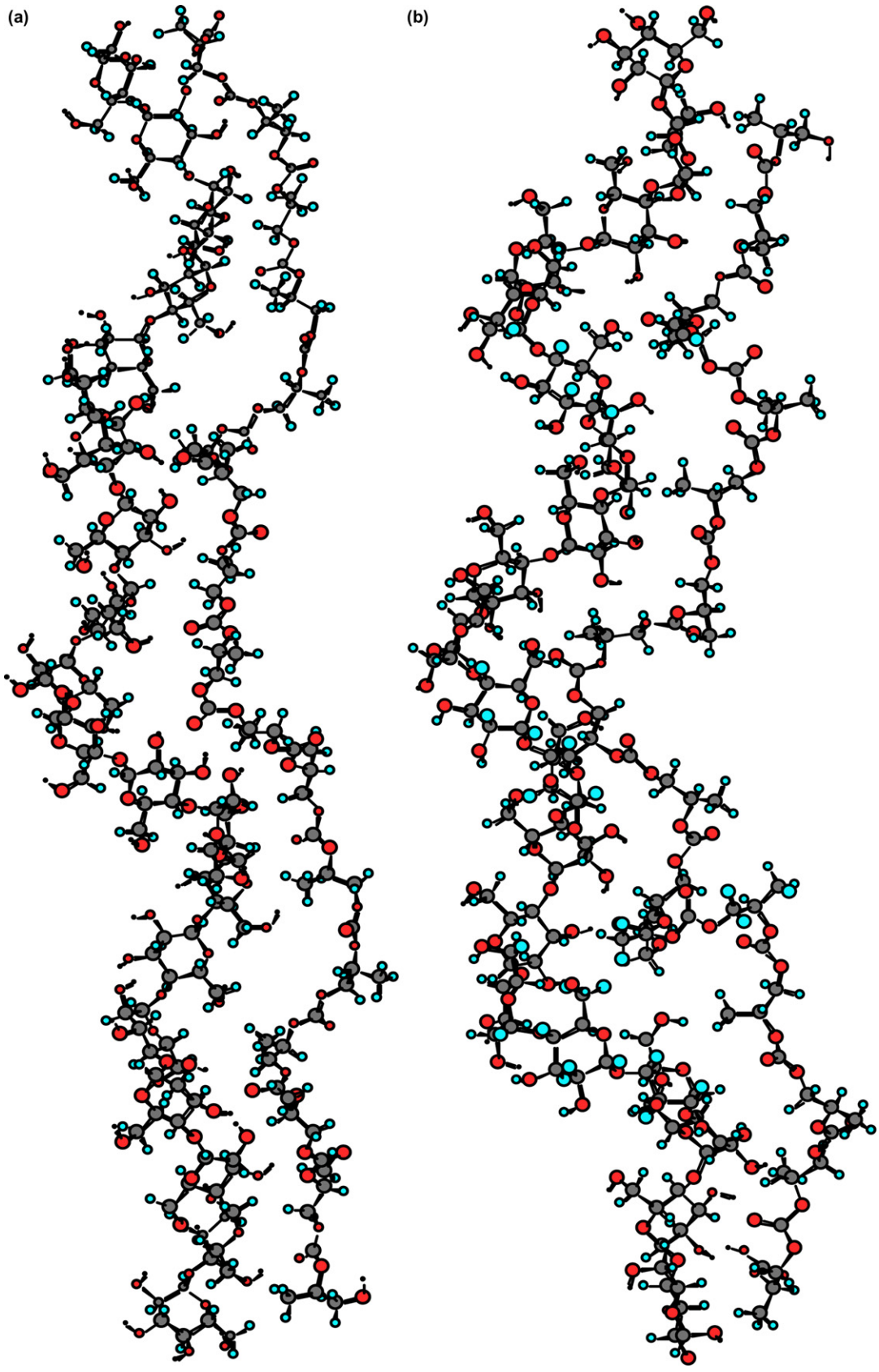

Fig. 6. Geometrically optimized structures of 20A:17P complexes at (a) AM1 and (b) PM3 levels.

Table 1
Binding energies ΔE (kJ/mol) at AM1, PM3 and B3LYP levels for the 1A:1P, 5A:5P, 10A:10P, 15A:15P and 20A:20P systems

	1A:1P	5A:5P	10A:10P	15A:13P	20A:17P
AM1	−22.43	−28.49	−16.83	−70.42	−106.61
PM3	−17.49	−12.13	−73.22	−49.50	−45.02
B3LYP	−61.59	−41.00 single point energy	–	–	–

AM1 results for the average binding energy per hydrogen bond are fairly unchanged and clustered around the average value of −12.76 kJ/mol with the standard deviation of 1.47 kJ/mol. PM3 results on the other hand cluster around the average value of −9.79 kJ/mol with a rather large standard deviation of 5.02 kJ/mol.

3.3. Vibrational frequency analysis

To gain further insight into the intermolecular interactions between the two polymers, a vibrational frequency analysis was carried out. The purpose of the analysis was twofold: (a) to obtain vibrational frequencies of the carbonyl C═O bond of PPC and the hydroxyl OH bond of amylose for the purpose of qualitative comparison with experimental IR spectra, and (b) to ascertain the located stationary points as true minima (all eigenvalues of the Hessian matrix are positive).

The vibrational frequencies were calculated at the AM1 and PM3 levels for the 1A:1P and 5A:5P complexes as the calculations for the remaining three systems were too expensive computationally. For similar reasons, the frequencies were computed at the B3LYP level only for the smallest 1A:1P system. The computed carbonyl C═O group frequencies of pure PPC, hydroxyl OH group frequencies of pure amylose, and the corresponding frequencies for the complexes are given in Tables 3 and 4. Both systems exhibit a decrease in the carbonyl and hydroxyl bond stretching frequencies in the complex as compared to the corresponding frequencies in PPC and amylose, respectively. This clearly indicates a specific interaction between the carbonyl group of PPC and the hydroxyl group of amylose. It can also be seen that the PM3 method overestimates the decrease in the frequencies as compared with the AM1 method.

Before attempting to compare these computed frequencies with the experimental results, it must be kept in mind that our current model simulates a simplified version of starch by modeling only the amylose portion. Thus, a quantitative comparison of the frequencies cannot be justified; nevertheless, a qualitative comparison can prove to be helpful to appreciate the nature of interactions between starch and PPC. Previous experimental FT-IR studies have been carried out on starch–PPC systems [24]. A close inspection of the FT-IR spectra shows a strong carbonyl stretching absorption at about 1754 cm^{-1} for PPC. Moreover, the absorption peak for the starch–PPC system (50/50) is shifted by about 13 cm^{-1} lower than that for PPC at 1741 cm^{-1} indicating a specific interaction between the carbonyl and hydroxyl groups. The experimental decrease of 13 cm^{-1} compares fairly well with our theoretically computed value of 10 cm^{-1} for the 5A–5P system at the PM3 level and 17 cm^{-1} for the 1A–1P complex at the AM1 level. The remaining computed decreases in frequencies are large compared to the experimental values; nonetheless, they do indicate the presence of favorable interactions between amylose and PPC.

The experimental FT-IR spectra also show an absorption peak at 3397 cm^{-1} for the hydroxyl OH group of starch, which is shifted by 6–3391 cm^{-1} for starch–PPC blend (50/50), indicating an interaction with the carbonyl C═O group of PPC. While the corresponding theoretically computed hydroxyl OH frequencies show a bigger offset as compared to the experimental values, the decrease in the hydroxyl OH frequencies

Table 2
Number of hydrogen bonds (N), average hydrogen bond distance (Å), number of hydrogen bonds per PPC monomer and average binding energy per hydrogen bond (kJ/mol) at the AM1 and PM3 levels for the 1A:1P, 5A:5P, 10A:10P, 15A:15P and 20A:20P systems

	Complex	Number of hydrogen bonds (N)	Average hydrogen bond distance (Å)	Number of hydrogen bonds per PPC monomer	Average binding energy per hydrogen bond (kJ/mol)
AM1	1A:1P	2	2.37	2	−11.21
	5A:5P	2	2.20	0.40	−14.23
	10A:10P	5	2.22	0.50	−14.10
	15A:13P	8	2.26	0.62	−13.68
	20A:17P	10	2.29	0.59	−10.67
PM3	1A:1P	1	1.81	1	−17.49
	5A:5P	3	2.59	0.60	−4.06
	10A:10P	5	2.66	0.50	−14.64
	15A:13P	7	2.22	0.54	−15.44
	20A:17P	8	2.26	0.48	−5.61

Table 3
Vibrational frequencies (cm^{-1}) of the carbonyl C═O group at the AM1, PM3 and B3LYP levels for 1P, 1A:1P, 5P and 5A:5P systems and their corresponding decrease in frequencies

	AM1	PM3	B3LYP
1P	2117	2003	1819
1A:1P	2100	1979	1771
Decrease	17	24	48
5P	2106	1977	–
5A:5P	2099	1967	–
Decrease	7	10	–

Table 4
Vibrational frequencies (cm^{-1}) of the hydroxyl OH group at the AM1, PM3 and B3LYP levels for 1A, 1A:1P, 5A and 5A:5P systems and their corresponding decrease in frequencies

	AM1	PM3	B3LYP
1A	3461	3890	3635
1A:1P	3434	3818	3422
Decrease	27	72	215
5A	3484	3890	–
5A:5P	3435	3841	–
Decrease	49	49	–

for both complexes at the AM1, PM3 and B3LYP levels does suggest a favorable interaction between amylose and PPC.

4. Conclusions

In this work, molecular modeling calculations employing the DFT based B3LYP and semi-empirical AM1 and PM3 methods were performed on five pairs of amylose–PPC complexes to investigate the nature of interactions between starch and PPC. The geometrically optimized structures of all complexes indicate formation of hydrogen bonds between amylose and PPC polymers. Owing to steric hindrance, the number of hydrogen bonds identified per PPC monomer decreases with increasing complex length and reaches an average saturation value of 0.51 for PM3 and 0.57 for AM1 for larger systems. The computed decrease in vibrational frequencies of carbonyl and hydroxyl groups in the complexes as compared to their corresponding pure PPC and amylose counterparts confirms the presence of specific interactions between amylose and PPC. The computed theoretical frequencies and their red shift agree at least qualitatively with the experimental results as far as the confirmation of favorable interactions between starch and PPC is concerned. Theoretical calculations thus performed provide useful insight into the nature of interactions between starch and PPC and prove the capability of quantum mechanical methods to model similar interactions.

References

[1] Qi Q, Wu Y, Tian M, Liang G, Zhang L, Ma J. Modification of starch for high performance elastomer. Polymer 2006;47:3896–903.

[2] Girija BG, Sailaja RRN, Madras G. Thermal degradation and mechanical properties of PET blends. Polymer Degradation and Stability 2005;90: 147–53.

[3] Szymanowski H, Kaczmarek M, Gazicki-Lipman M, Klimek L, Wozniak B. New biodegradable material based on RF plasma modified starch. Surface and Coatings Technology 2005;200:539–43.

[4] Shah PB, Bandopadhyay S, Bellare JR. Environmentally degradable starch filled low density polyethylene. Polymer Degradation and Stability 1995;47:165–73.

[5] Willett JL, Felker FC. Tensile yield properties of starch-filled poly(ester amide) materials. Polymer 2005;46:3035–42.

[6] Godbillot L, Dole P, Joly C, Roge B, Mathlouthi M. Analysis of water binding in starch plasticized films. Food Chemistry 2006;96:380–6.

[7] Bangyekan C, Aht-Ong D, Srikulkit K. Preparation and properties evaluation of chitosan-coated cassava starch films. Carbohydrate Polymers 2006;63:61–71.

[8] Mali S, Sakanaka LS, Yamashita F, Grossmann MVE. Water sorption and mechanical properties of cassava starch films and their relation to plasticizing effect. Carbohydrate Polymers 2005;60:283–9.

[9] Wu CS. Physical properties and biodegradability of maleated-polycaprolactone/starch composite. Polymer Degradation and Stability 2003; 80:127–34.

[10] Godbole S, Gote S, Latkar M, Chakrabarti T. Preparation and characterization of biodegradable poly-3-hydroxybutyrate–starch blend films. Bioresource Technology 2003;86:33–7.

[11] Parra DF, Tadini CC, Ponce P, Lugão AB. Mechanical properties and water vapor transmission in some blends of cassava starch edible films. Carbohydrate Polymers 2004;58:475–81.

[12] Khan MA, Bhattacharia SK, Kader MA, Bahari K. Preparation and characterization of ultra violet (UV) radiation cured bio-degradable films of sago starch/PVA blend. Carbohydrate Polymers 2006;63: 500–6.

[13] Lu Y, Weng L, Cao X. Morphological, thermal and mechanical properties of ramie crystallites—reinforced plasticized starch biocomposites. Carbohydrate Polymers 2006;63:198–204.

[14] Shujun W, Jiugao Y, Jinglin Y. Preparation and characterization of compatible thermoplastic starch/polyethylene blends. Polymer Degradation and Stability 2005;87:395–401.

[15] Guohua Z, Ya L, Cuilan F, Min Z, Caiqiong Z, Zongdao C. Water resistance, mechanical properties and biodegradability of methylated-cornstarch/poly(vinyl alcohol) blend film. Polymer Degradation and Stability 2006;91:703–11.

[16] Xu YX, Kim KM, Hanna MA, Nag D. Chitosan–starch composite film: preparation and characterization. Industrial Crops and Products 2005; 21:185–92.

[17] Huang CY, Roan ML, Kuo MC, Lu WL. Effect of compatibiliser on the biodegradation and mechanical properties of high-content starch/low-density polyethylene blends. Polymer Degradation and Stability 2005; 90:95–105.

[18] Gaspar M, Benko Z, Dogossy G, Reczey K, Czigany T. Reducing water absorption in compostable starch-based plastics. Polymer Degradation and Stability 2005;90:563–9.

[19] Lu Y, Tighzert L, Dole P, Damien E. Preparation and properties of starch thermoplastics modified with waterborne polyurethane from renewable resources. Polymer 2005;46:9863–70.

[20] Chen L, Ni Y, Bian X, Qiu X, Zhuang X, Chen X, et al. A novel approach to grafting polymerization of ε-caprolactone onto starch granules. Carbohydrate Polymers 2005;60:103–9.

[21] Chen L, Qiu X, Deng M, Hong Z, Luo R, Chen X, et al. The starch grafted poly(L-lactide) and the physical properties of its blending composites. Polymer 2005;46:5723–9.

[22] Santos PV, Oliveira LM, Cereda MP, Alves AJ, Scamparini ARP. Mechanical properties, hydrophilicity and water activity of starch-gum films: effect of additives and deacetylated xanthan gum. Food Hydrocolloids 2005;19:341–9.

[23] Ge XC, Li XH, Zhu Q, Li L, Meng YZ. Preparation and properties of biodegradable poly(propylene carbonate)/starch composites. Polymer Engineering and Science 2004;44(11):2134–40.

[24] Weimann PA, Jones TD, Hillmyer MA, Bates FS, Londono JD, Melnichinko Y, et al. Phase behavior of isotactic polypropylene–poly-(ethylene/ethylethylene) random copolymer blends. Macromolecules 1997;30:3650–7.

[25] Reichart GC, Graesseley WW, Register RA, Krishnamoorti R, Lohse DJ. Anomalous attractive interactions in polypropylene blends. Macromolecules 1997;30:3036–41.

[26] Masson JF, Collins P, Robertson G, Woods JR, Margeson J. Thermodynamics, phase diagrams, and stability of bitumen-polymer blends. Energy and Fuels 2003;17:714–24.

[27] Schweizer K, Curro JG. Integral equation theory of the structure and thermodynamics of polymer blends. Journal of Chemical Physics 1989;91(8):5059–81.

[28] Chatterjee AP. Integral equation theory for athermal solutions of linear polymers. Journal of Chemical Physics 2004;121(22):11432–9.

[29] Pesci AI, Freed KF. Lattice theory of polymer blends and liquid mixtures: beyond the Flory–Huggins approximation. Journal of Chemical Physics 1989;90(3):2017–26.

[30] Dudowicz J, Freed KF. Effect of monomer structure and compressibility on the properties of multicomponent polymer blends and solutions: 1. Lattice cluster theory of compressible systems. Macromolecules 1991; 24:5076–95.

[31] Dudowicz J, Freed KF. Lattice cluster theory for pedestrian. 2. Random copolymer systems. Macromolecules 2000;33:3467–77.

[32] Genovese A, Shanks RA. Simulation of the specific interactions between polyamide-6 and a thermoplastic polyurethane. Computational and Theoretical Polymer Science 2001;11:57–62.

[33] Dewar MJS, Zoebisch EG, Healy EF, Stewart JJP. AM1: a new general purpose quantum mechanical molecular model. Journal of the American Chemical Society 1985;107(13):3902–9.

[34] Stewart JJP. Optimization of parameters for semiempirical methods. Journal of Computational Chemistry 1989;10:209–21.
[35] Hyperchem™ release 7.52, Windows molecular modeling system. hypercube, Inc.; 2002.
[36] Becke AD. Density-functional exchange-energy approximation with correct asymptotic behavior. Physical Review A 1988;38(6):3098–100.
[37] Lee C, Yang W, Parr RG. Development of the Colle–Salvetti correlation-energy formula into a functional of the electron density. Physical Review B 1988;37(2):785–9.
[38] Becke AD. Density-functional thermochemistry. III. The role of exact exchange. Journal of Chemical Physics 1993;98(7):5648–52.
[39] Frisch MJ, Trucks GW, Schlegel HB, Scuceria GB, Robb MA, Cheeseman JR, et al. Pittsburgh, PA: Gaussian Inc.; 1998.